International Journal of Concrete Structures and Materials

RESEARCH Open Access

Performance Evaluation of Torque-Controlled Expansion Anchors with Improved Sleeve and Header Details

Moo-Won Hur[2], Kyoung-Hun Chae[1], Hyun-Ho Lee[2] and Tae-Won Park[1*]

Abstract

This study assesses improvements in the head and extension sleeve parts for a post-installed anchor. The sleeve and head details were proposed to enhance the structural performance of the post-installed anchor, and the optimal structural shape was determined through finite element analysis. The analysis results revealed that the anchor's performance was most efficiently improved when the sleeve length was 9.0 mm and the head length was 3.0 mm. In the model with these dimensions applied, the performance improved approximately 1.71 times compared to the existing model, validating the effectiveness of the proposed structural details. The improved pull-out strength test of anchor diameter M12 showed an increase of 1.25 times in normal-strength concrete and 1.28 times in high-strength concrete, with an embedded depth of 50 mm. The improved pull-out strength test of anchor diameter M16 showed that the pull-out strength increased by 1.42 times for normal-strength concrete and about 1.33 times for high-strength concrete. This research proposes a modified equation that reflects changes in the effective embedded depth and diameter. A comparison of the proposed equation with that of European Technical Approval Guideline (ETAG) showed that the correlation coefficient changed from 0.908 to 0.962, and the coefficient of variation changed from 18.9 to 10.4%, meaning that the proposed equation reflected the actual experimental values more accurately.

Keywords Concrete cone failure, Design equation, FEM analysis, Header length, Post-installed anchor, Shear strength, Sleeve length, Tensile strength

1 Introduction

Concrete anchors can be divided into cast-in anchors, which are installed before concrete pouring as shown in Fig. 1, and post-installed anchors, which are installed after the concrete has hardened. Cast-in anchors become integrated with the concrete as it hardens, offering excellent anchorage and load transfer performance, but they have the disadvantage of being prone to construction errors and difficult to modify. On the other hand, post-installed anchors, while slightly inferior in structural performance to cast-in anchors allow for flexible positioning and modification according to construction purposes, making them widely used in various construction sites. Typical examples of post-installed anchor applications include fixing curtain walls, seismic reinforcement, securing attachments for bridges and tunnels, and fixing equipment and facilities (Fig. 2).

The performance details for the design standards of post-installation anchors are provided in the American Concrete Institute (ACI) code and Euro code (Institute and (ACI) Committee, 2019; ACI Committee, 2019; ACI

Journal information: ISSN 1976-0485 / eISSN 2234-1315.

*Correspondence:
Tae-Won Park
tw001@dankook.ac.kr
[1] Department of Architectural Engineering, Dankook University, Yongin, Republic of Korea
[2] Department of Smart Architecture Engineering, Dongyang University, Yeongju-Si, Republic of Korea

Committee et al., 2011). In Korea, the anchor design method is denoted in the appendix of the Korean Building and Commentary (Korean Building Code and Commentary (KBC) 2016), based on ACI 318-19 (Table 1) (ACI Committee, 2019).

As earthquakes are occurring with greater frequency and with growing scale, interest in reinforcing the seismic performance of buildings is also increasing. Earthquake damage to buildings leads to casualties and economic losses that are difficult to recover from (Fig. 3).

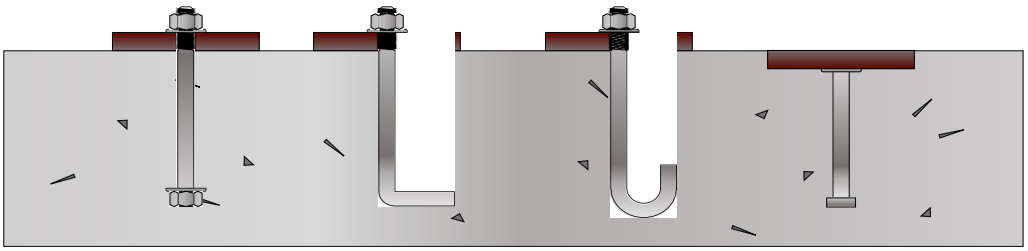

(a) Cast-in anchors

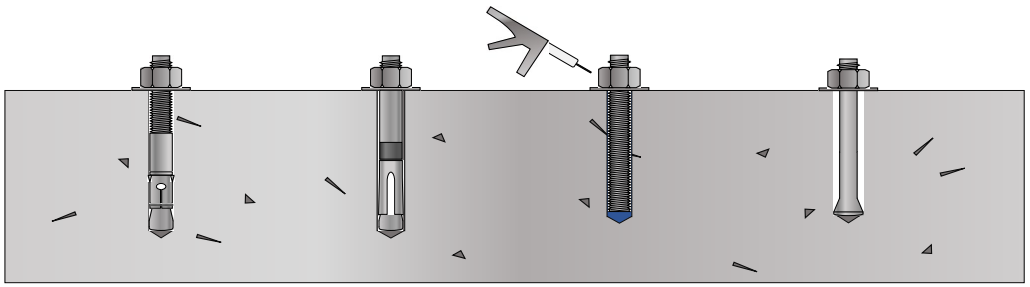

(b) Post-installed anchors

Fig. 1 Types of anchors (ACI 355.2 figure reconstruction)

Fig. 2 Applications of post-installed anchors

Table 1 Standards regarding post-installation anchors for concrete

Content	National anchor design standards and methods by country
USA	• ACI Committee 318 (2019) Building Code Requirements for Structural Concrete • ACI Committee 355.2 (2019) Qualification of Post-installed Mechanical Anchors in Concrete (ACI 355.2-19) and Commentary • ASTM E488 Standard Test Methods for Strength of Anchors in Concrete and Masonry Elements
Europe region	• EOTA (2013) Guideline for European Technical Approval of Metal Anchors for Use in Concrete – Annex C: Design Methods for Anchorage (ETAG 001)
Korea	• KCI (2021) Anchor Design Code for Concrete (KDS 14 20 54). Sejong, Korea: Ministry of Land, Infrastructure and Transport (MOLIT), Korea Concrete Institute (KCI)

Fig. 3 Example of earthquake damage. Source: Architectural Institute of Korea (ACI), damage to non-structural materials described in the Pohang earthquake report, https://www.aik.or.kr/html/page05_05.jsp

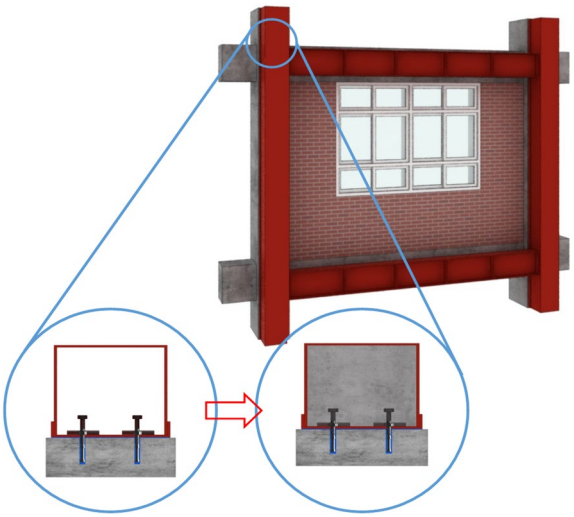

Fig. 4 CFT (concrete filled steel tube) seismic reinforcement

Therefore, it is very important to reinforce old buildings to improve their seismic performance by attaching a member with high rigidity and strength to an existing member to support aged concrete rather than directly reinforcing the rigidity and strength of the structural members. In most cases, post-installed anchors are recommended between the reinforcing material and the existing member (Fig. 4). Therefore, the performance of the anchor must be verified to ensure quality control for seismic reinforcement (AIK 2016).

As previously described, post-installed anchors are being utilized for a variety of purposes and numerous studies related to them are being conducted. The research trends associated with post-installed anchors are as follows. Research trends for post-installed anchors emphasize finite element analysis of the nonlinear tensile behavior characteristics of the torsion-controlled expansion anchors (Dassault Systemes, 1978). The anchor depth and torque values are tested to present a load–displacement model (Breen et al., 2001). Nonlinear finite element analysis studies elucidate the fracture tendency of anchors and the degree of damage to concrete due to external loads (ETAG, 2003; European Technical Approval Guideline (ETAG), 1997; Delhomme et al., 2018). The resistance performance is then evaluated by performing static and dynamic tests on specimens not affected by the edge distance to assess the behavior of a single anchor based on the presence or absence of cracks in the concrete (Alhaidary & Al-Tamimi, 2021). The internal force is then confirmed from the tensile test using the edge distance as the main variable (Gontarz & Podgorski, 2019). For example, Kim et al. (2013) (Lubliner et al., 1989) conducted a finite element analysis to compare the effect on torque for post-installed anchors used in structures in Korea. Chen et al. (2020) (Bang et al., 2010) investigated the pull-through (PT) and pull-out (PO) failure modes of torque-controlled expansion (TCE) anchors and developed an empirical model for N_p. Pishro et al. (2020) (Kim et al., 2013) analyzed local bond stress (LBS) between ultra-high-performance concrete (UHPC) and reinforcing steel bars, proposed a comprehensive LBS equation, and validated it with experimental and numerical results. Alhaidary et al. (2021) (Tsavdaridis et al., 2016) studied the pull-out performance of ETA-approved and non-ETA-approved anchors in the Middle East. They found that ETA-approved anchors were more robust under suboptimal site conditions. Siamakani et al. (2022) (Korean Building Code and Commentary (KBC)

2016) found that PRs can prevent concrete breakout failures caused by expansion anchors.

Based on the existing literature and data on post-installed anchors, the key research objectives of this study are as follows. The performance of post-installed anchors in concrete is significantly influenced by the frictional area between the anchor and the concrete. The factors affecting this frictional area mainly originate from the structural details of the anchor, which can be improved to enhance performance. In this study, we improved the structural details of the anchor to secure a sufficient frictional area and verified their performance through analysis and experimentation. The innovation and contribution of this research can be summarized as follows. Firstly, the structural details of the anchor have been improved to enhance the anchor's performance, thereby resulting in a more stable resistance against concrete. This research can serve as a foundation for enhancing the performance of anchors. Moreover, this study, with the support of both analytical and experimental evidence, confirms the crucial role of the frictional area in improving the performance of anchors. Consequently, this factor should be considered in future research endeavors related to anchor performance in concrete.

2 Mechanical Anchor Performance

2.1 Performance of the Post-installed Anchor

In this study, we aim to propose structural details to improve the structural performance of existing anchors, focusing on torque-controlled expansion anchors among mechanical post-installed anchors. Torque-controlled expansion anchors are anchored in concrete through the pressure generated by the expansion of the sleeve and the frictional force between the concrete and the sleeve. The load and anchoring mechanism of the anchor are illustrated in Fig. 5.

To improve the structural performance of post-installed anchors, we must first examine the process of internal force transmission in the anchor, as shown in Fig. 5. The anchor strength is mainly determined by the degree of increase in the frictional force with concrete in the head of the anchor body and the expansion degree of the sleeve coupled with the body. In other words, when the anchor is bonded to the concrete, the sleeve is pushed into the head part and becomes integrated. The degree of friction and grip that this integrated part exerts within the concrete determines the pull-out strength of the anchor. When the length of the anchor head expands, as shown in Fig. 6, the frictional force and the keying between the anchor and the concrete surface increase, and the sleeve further expands as the load is applied, which in turn is expected to improve the overall drawing

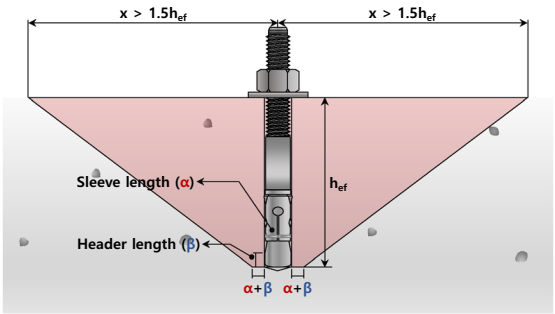

Fig. 6 Expected concrete cone fracture area due to improvements in sleeve and head details

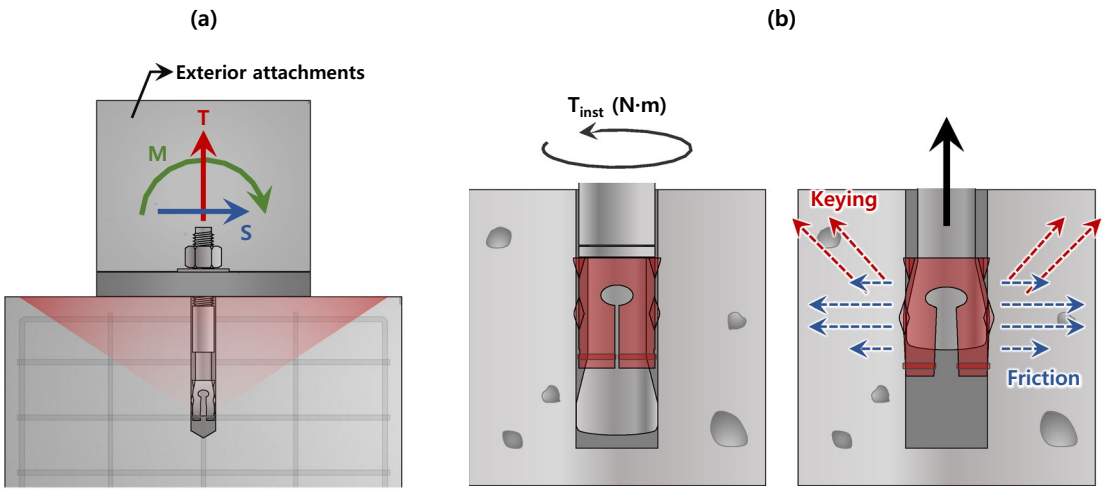

Fig. 5 Behavioral characteristics of torque-controlled expansion anchors: **a** load resistance mechanism, **b** anchorage mechanism

performance. Furthermore, the angle between the fracture surface of the anchor and the concrete surface is reduced, which reduces the destruction area of the concrete cone.

In this study, we aim to enhance the structural details of existing post-installed anchors and to verify these improvements (Fig. 7). Initially, we plan to study the anchoring and load mechanisms of post-installed anchors through existing literature and materials, and propose structural details to improve the anchors' performance. Using the sleeve and head details as variables, we will conduct finite FEM analysis and aim to derive the optimal structural shape for the anchor based on the analysis results. Finally, we intend to fabricate a prototype of the anchor, perform performance verification tests, and, based on the experimental results, propose a new anchor design formula to evaluate the performance of the developed anchor, ensuring the sentences flow naturally.

2.2 Anchorage Mechanism of Post-installed Anchors

The contact stress between post-installed anchors and concrete is a crucial mechanism for securing the anchor within the concrete. Contact stress occurs at the interface between the anchor and the concrete and is influenced by several factors. Firstly, the strength of both the anchor and concrete significantly impacts the contact stress. When the sleeve of the post-installed anchor expands, if the material strength of the anchor is low, the resistance to the concrete's compressive strength may be insufficient, leading to deformation in the steel. Conversely, if the compressive strength of the concrete is low, it may be unable to accommodate the steel strength of the anchor, resulting in concrete splitting or cracking. Therefore, to ensure the appropriate contact stress, the strength of both the anchor and the concrete must be adequately considered. Secondly, the bond strength between the anchor and the concrete is related to contact stress. The stronger the bond, the more evenly the stress applied to the concrete is distributed, resulting in a uniform stress distribution. This ensures anchor safety and prevents potential issues concerning performance deviation in the anchor system.

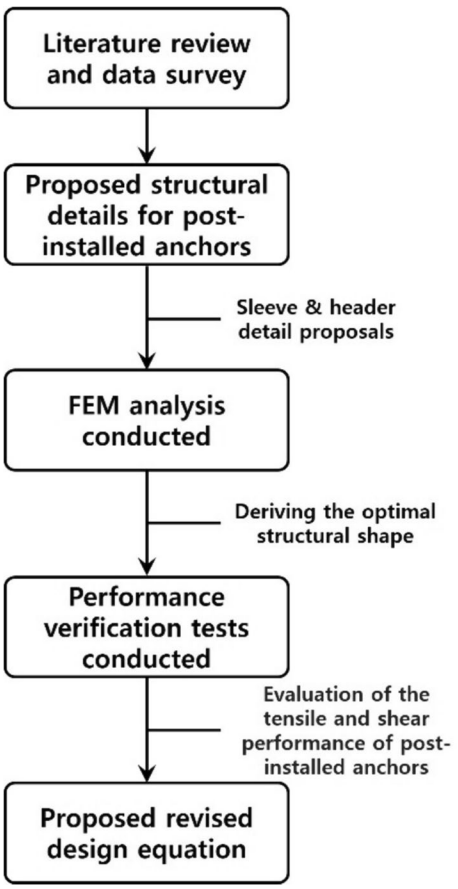

Fig. 7 Research flow-chart

2.3 Destruction Mechanism for the Post-installed Anchor

A post-installed anchor is a structural material that transmits the load acting on the external attachments installed in existing concrete structures to the base material. Recently, as the importance of reinforcing concrete structures has increased, evaluation to ensure the performance of post-installed anchors has become very important. Even though it is safe to bury the anchor when pouring concrete, post-installed anchors are widely used due to the conversion of construction methods, ease of selecting anchor embedding locations, and design and construction conditions modified by the additional structural reinforcement.

Fig. 8 illustrates the failure modes of a post-installed anchor under tensile load, and the smallest value of the failure strengths can be determined and used as the design strength of the post-installed anchor.

The most representative failure mode of a post-installed anchor under tensile load is concrete breakout failure. This type of failure occurs when the embedment depth of the anchor is insufficient to cause steel failure, resulting in the anchor breaking out in a conical cone shape along with a portion of the surrounding concrete. The failure strength of concrete breakout can be calculated based on the concrete's compressive strength and the effective embedment depth, as shown in Eqs. (1) and (2), and is specified in ACI 355.2-19:

$$N_{cb} = \frac{A_{Nc}}{A_{Nco}} \psi_{ed,N} \psi_{c,N} \psi_{cp,N} N_b, \quad (1)$$

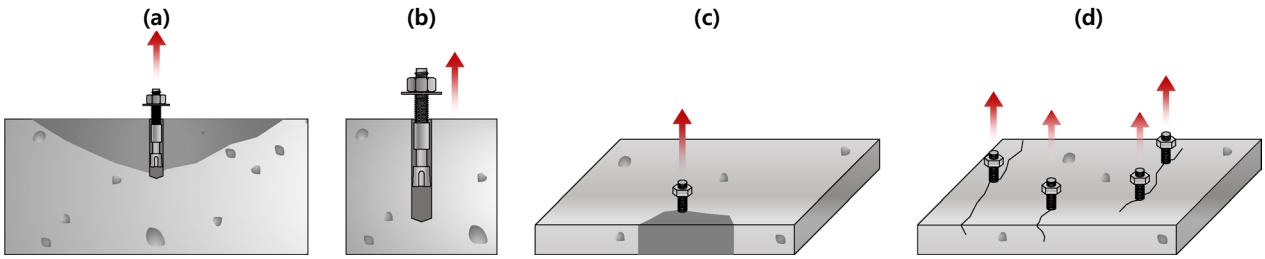

Fig. 8 Failure mode of the anchor: **a** concrete breakout, **b** pull-out failure, **c** side-face blowout, **d** concrete splitting

$$N_b = k_c \sqrt{f_{ck}}\, h_{ef}{}^{1.5}, \tag{2}$$

where $\Psi_{ed,N}$ denotes the modification coefficient by edge distance; $\Psi_{c,N}$ denotes the modification coefficient by cracks in base concrete; $\Psi_{cp,N}$ denotes anchor installation point of base concrete; A_{Nc} denotes the projected area of base concrete; A_{Nco} denotes the projected area of anchor fracture surfaces (edge distance $1.5h_{ef}$ or more); N_b denotes the characteristic tensile capacity of an anchor with a concrete failure mode. In relation to the base concrete strength; k_c denotes the base concrete failure strength coefficient (tensile); f_{ck} denotes the concrete compressive strength design criteria; and h_{ef} denotes the effective burying depth of the anchor.

3 Geometric Suggestions to Improve Anchor Performance

3.1 Proposed Structural Details of Post-installed Anchors

In this study, we aim to improve the structural performance of post-installed anchors by enhancing the sleeve and head details of the existing anchors. As described in Sect. 2.1, improving the sleeve and head details can enhance the expansion force of the sleeve acting on the concrete, and also improve the frictional force between the concrete and the sleeve, thereby enhancing the overall bearing capacity of the anchor. Based on this structural theory, we have illustrated the detailed improvements for the sleeve and head of the existing post-installed anchors in Fig. 9, and aim to derive the optimal structural shape with the best internal strength of the post-installed anchors through finite element analysis.

3.2 Finite Element Method (FEM) Analysis Parameter Setting

As shown in Fig. 10a, the post-installed anchor has a screw thread, a washer, and a nut at one end, and at the other end, it has a structure where an expansion header and an expansion sleeve are hung by processing a thread. The post-installed anchor can resist a tensile strength with jamming and frictional forces, and the parameters that can affect such tensile strength include the length of the sleeve and the length of the header (Fig. 10b). Therefore, this study performs a numerical analysis by setting the basic model and six analysis variables for the anchor diameter M12 anchor, as shown in Table 2, to select the optimal sleeve length and header length. Tables 3 and 4 show the details of the mesh and material used in the FEM analysis. ABAQUS software (version 6.2) (Bang et al., 2010) was used for the analysis (Kim et al., 2013).

The finite element analysis in this study was performed using ABAQUS. In order to improve the drawing performance of the anchor, a direct parameter capable of increasing the friction force was used. The sleeve shape and head length were used as variables during the analysis. Fig. 10b shows the existing and improved shape of the installation anchor after the sleeve and head details,

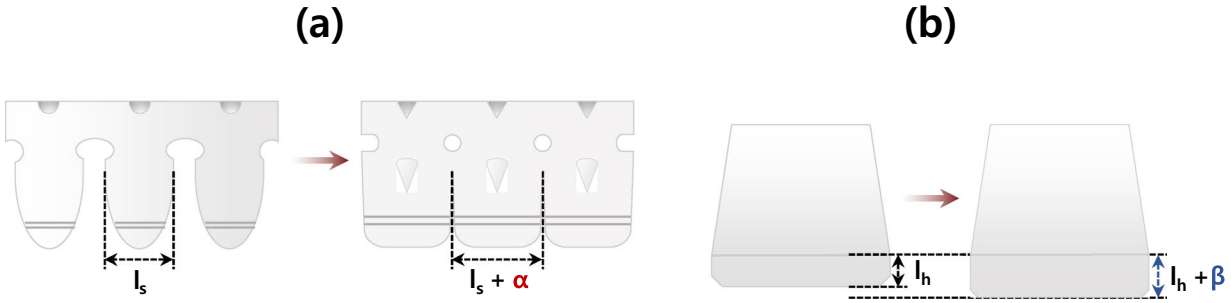

Fig. 9 Sleeve and header detail proposal: **a** sleeve detail, **b** header detail. Here, l_s in **a** represents the sleeve length of the existing anchor, and α denotes the increased sleeve length, while l_h in **b** represents the head length of the existing anchor, and β denotes the increased head length

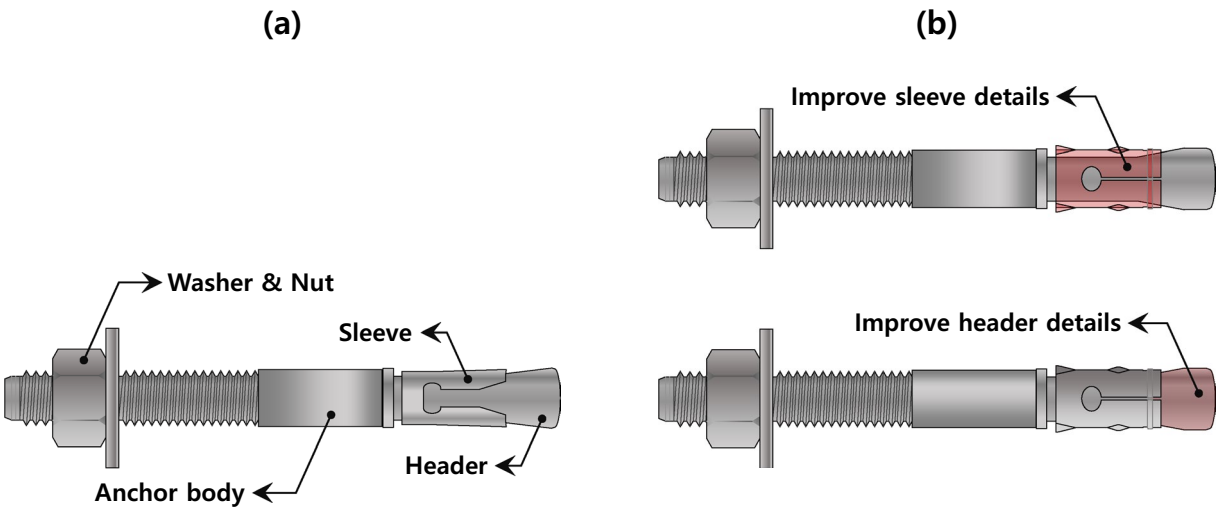

Fig. 10 Shape of anchor: **a** before and **b** after

Table 2 Analysis variables (unit: mm)

Content	Case-1	Case-2	Case-3	Case-4	Case-5	Case-6	Case-7
Sleeve length	6.4	8.0	9.0	10.0	6.4	6.4	6.4
Header length	0.94	0.94	0.94	0.94	1.50	3.00	4.50

Table 3 Mesh and material details for FEM analysis

Mesh detail values		Material detail values	
Item	**Content**	**Item**	**Content**
Mesh type	Solid mesh	Model type	Linear elastic isotropic
Mesh used	Curvature based mesh	Default failure criterion	Max von Mises stress
Jacobian points	4 Points	Yield strength	250 MPa
Maximum element size	2.0047 mm	Tensile strength	400 MPa
Tolerance	0.100235 mm	Elastic modulus	200,000 MPa
Mesh quality	High	Poisson's ratio	0.26
Failed remesh parts with incompatible mesh	Off	Mass density	7850 g/cm^3
		Shear modulus	79,300 MPa

Table 4 FEM results (comparison of pull-out load relative to each case)

Content	FEM analysis variables						
	Case-1	Case-2	Case-3	Case-4	Case-5	Case-6	Case-7
Parameter	Original	*Sleeve length*			*Header length*		
		8.0 mm	9.0 mm	10.0 mm	1.5 mm	3.0 mm	4.5 mm
Load (kN)	23.2	25.6	28.2	28.9	30.2	33.1	33.4
Relative ratio	1.00	1.11	1.21	1.25	1.30	1.43	1.44

developed in this study, were improved. The case parameters for finite element analysis are shown in Table 2. Case 1 is the structural shape of the existing anchor, cases 2 to 4 are to derive the optimal length of the sleeve, and cases 5 to 7 are to derive the length of the head. Finally, in case 8, the case with the most efficient structural performance of the sleeve and head is selected and collected, and then the optimal shape is determined. The mesh details for finite element analysis of the post-installed anchor are as follows. The rear installation anchor has a sleeve surrounding the anchor shaft. Since it consists of a continuous body, a solid mesh was applied. In addition, the overall shape of the rear installation anchor consists of curvature.

Accordingly, a "curvature-based mesh" was used to form sufficient elements to increase the accuracy of interpretation. The model for the post-installed anchor is complicated because all elements are composed of curvature. Accordingly, to increase the accuracy of the analysis, the maximum size of the mesh was set to 2.0047 mm. In addition, the analysis was performed using the "Linear Elastic Isotropic" model to consider only the elastic deformation of steel because it is necessary to examine whether a uniform friction area acts on the sleeve through stress distribution. The yield strength (250 MPa) and tensile strength (400 MPa) of the material were applied with ASTM Steel's "ASTM A36," which is most similar to the steel strength of the actual anchor. The elastic modulus (E_s) of the material was 200,000 MPa, and the Poisson ratio was 0.26. In addition, von Mises was applied to define the yield of anchor steel in consideration of the three-dimensional stress state of the material. Since the tensile force acts along the anchor axis of the post-installed anchor, the analysis was performed by constraining the anchor's sleeve and then performing displacement control on the anchor axis. The method of applying loads and boundary conditions for post-installed anchors is as follows. The anchor is subjected to displacement control in the axial direction of the anchor body to determine its maximum load capacity. In particular, to verify whether the improved sleeve exhibits a uniform stress distribution surface, the friction coefficient between the anchor and the sleeve was set to 0 when defining the boundary conditions.

3.3 Finite Element Method (FEM) Analysis Results

Fig. 11 illustrates the results for each variable (sleeve length and header length) as a relative ratio of the basic model. In addition, Table 4 shows the results for each analysis variable. As shown in Fig. 11, a greater sleeve length resulted in a greater frictional force. However, the increase in the internal force decreased as the length of the sleeve exceeded 10.0 mm. The internal force increased linearly with the head length up to 3.0 mm, but the internal force did not significantly increase thereafter once the head length reached 4.5 mm.

Fig. 11 shows the relative ratio of the anchor's strength improvement due to the enhancement of sleeve and head length compared to the existing model. As seen in (a), as the sleeve length increases, the strength improves due to the increased friction area, but the increase in strength diminishes beyond 10.0 mm. The configuration of the sleeve allows for controlling the deformation of the steel within the elastic range by maintaining a certain distance between sleeves. However, if the sleeve length increases excessively, the distance between sleeves narrows, causing interference, and thus expansion of the sleeve does not occur even at the proper torque value, leading to a decrease in strength. Therefore, the optimal length of the sleeve was determined to be 9.0 mm, where the effect of enhancing the anchor's strength is most efficiently secured. In (b), it is observed that the anchor's strength

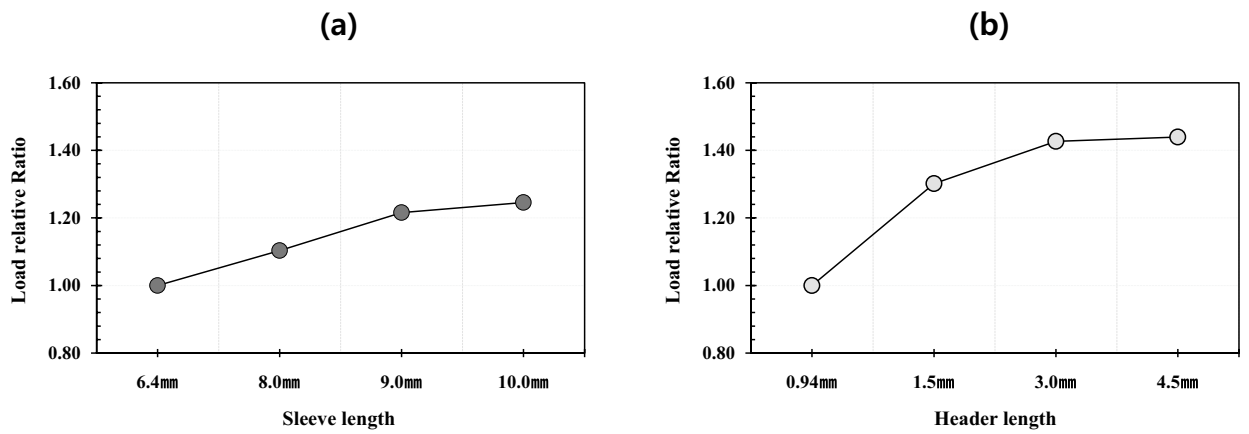

Fig. 11 Load relative ratio: **a** sleeve length, **b** header length

improves as the head length increases, but the additional improvement becomes limited beyond 3 mm. The combination of head and sleeve increases friction and tensile stress within the concrete, enhancing the anchorage performance. However, too long a head can cause local stress concentration in relatively short sleeves, damaging the material, and the elongation of the load transfer path can lead to a decrease in strength due to load dispersion. Thus, the optimal length of the head was determined to be 3.0 mm, where the effect of enhancing the anchor's strength is most efficient (Table 5) (Fig. 12).

4 Performance Evaluation of the Improved Post-installed Anchor

4.1 Structural Performance Tests for the Improved Post-installed Anchor

Structural performance tests were conducted to compare and analyze the performance of post-installed anchors (M12, M16, M20) with improved structural details based on the results of finite element analysis. The concrete specimens, that were made without reinforcing bars to prevent them from affecting the concrete breakout failure of the anchors, were fabricated as uncracked concrete measuring 1800 × 1800 × 300 mm, as shown in Fig. 13. The specimens were manufactured with a thickness of $h_{min} = 1.5h_{ef}$ or more, and the anchors were installed with a minimum anchor spacing of $s_{min} = 6d_0$ or more to prevent splitting and ensure that they did not affect each other (Fig. 13). The normal-strength of concrete was rated at 21 MPa, and the high-strength at 50 MPa. The compressive strength test after 28 days showed a normal-strength result of 23.5 MPa, and a high-strength result of 50.5 MPa.

The evaluation of anchor performance before and after improvement is shown in Table 6. The experiment consisted of an experimental group under the same conditions before and after the improvement. The post-installed anchor system was evaluated through a single anchor test, and the test was named as the concrete strength-effective embedded depth, according to the anchor improvement. For the standard experiment, at least five anchor specimens were produced per group according to the regulations, and these were evaluated by the mean value, standard deviation, and coefficient of variation. To satisfy these conditions, a performance evaluation was conducted on a total of 80 specimens,

Table 5 Optimal design results

Content	Case-1	Case-8
Parameter	Original model	Optimal model
Load (kN)	23.2	39.6
Load relative ratio	1.00	1.71

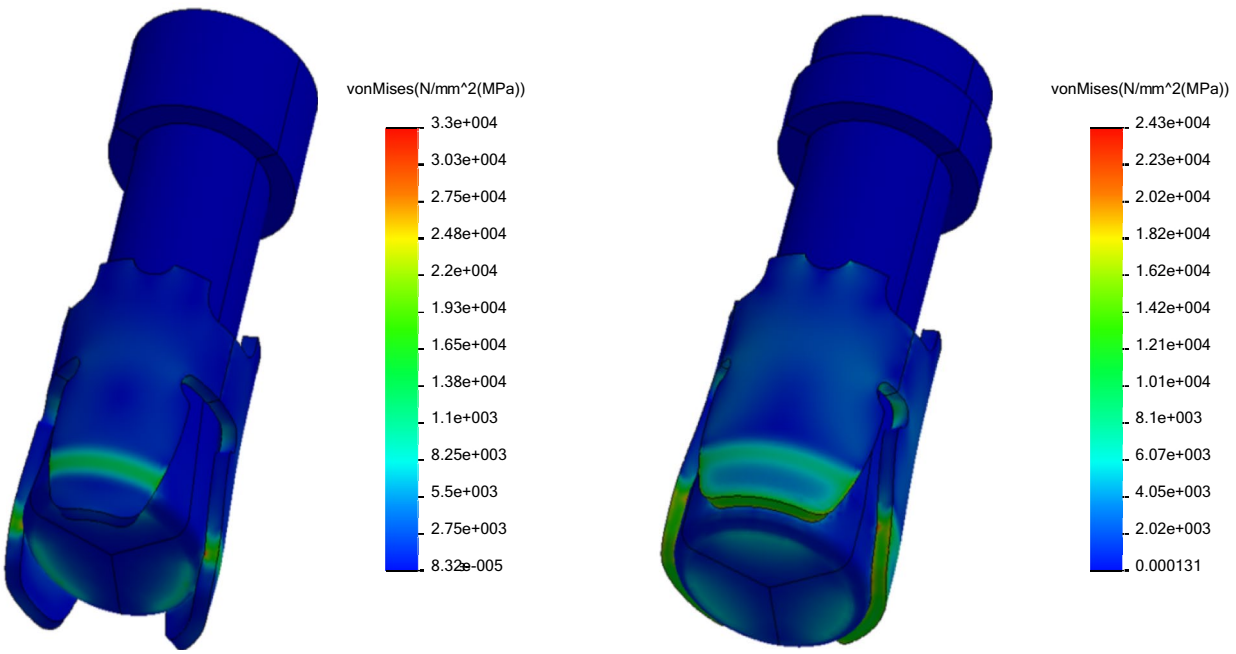

(a) Case-1 (Original model) (b) Case-8 (Optimal model)

Fig. 12 Analysis result

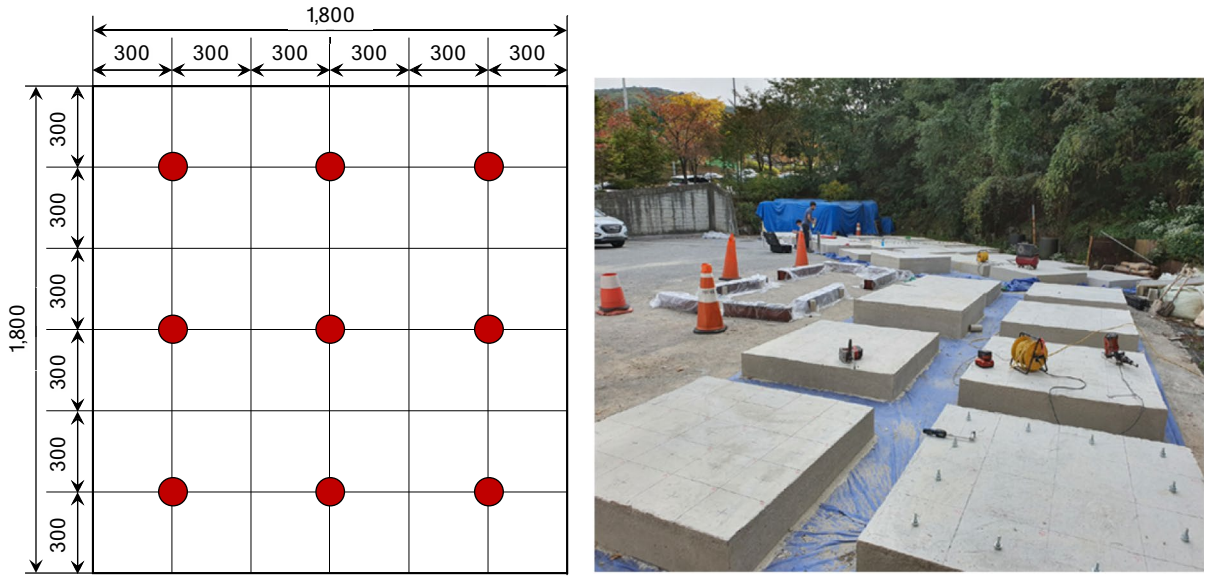

Fig. 13 Specimen preparation (unit: mm)

including 80 extraction tests and 30 shear tests, by classifying the parameters as anchor improvement, embedded depth, and concrete strength.

As shown in Table 6, these variables were accounted for because the relationship between the post-installed anchor and the concrete adhesion stress has a significant impact on the experimental results. The existing post-installed anchors were not able to sufficiently secure the anchor's bearing capacity as the concrete compressive strength increased. The sleeve of the existing post-installed anchor has a short length, which increases the possibility of steel deformation during expansion, therefore, it cannot receive constant expansion force or fully secure the anchor's bearing capacity. However, in the case of the developed post-installed anchor, there is no concern regarding steel deformation during expansion due to the longer sleeve length and the increased friction area of the sleeve as the length of the head increases, resulting in excellent bearing capacity.

Fig. 14 shows the setting diagram of the anchor pull-out test and shear tests. The connecting hardware was fastened to the anchor and installed so that the anchor was located at the center of the jig. After the jig was coupled to the load cell (500 kN), the cylinder was installed on the load cell and the anchor–jig–load cell was integrated with the full threaded bolt (M24). A linear variable displacement transducer (200 mm) was fixed to a jig to measure the displacement, and after connecting a hydraulic jack (250 kN) to apply a load, the load was measured with a load cell. Torque (50 N·m) was then applied for 10 min and the load was completely removed, followed by 50% of the torque being reapplied.

Table 6 Test variables

Type	Concrete strength	Diameter (mm)	Effective embedded depth (mm)
Pull-out	Normal-strength concrete	12	50, 70
		16	80
		20	100
	High-strength concrete	12	50, 70
		16	80
		20	100
Shear	Normal-strength concrete	12	70
		16	80
		20	100

4.2 Experimental Results and Analysis

Figs. 15 and 16 show the final failure photo of the anchor extraction test before and after the improvement. Tables 7 and 8 show the results of the test according to the concrete strength and embedded depth before and after the improvement of the M12 anchor. As shown in Fig. 15, the fracture area of the anchor before the improvement was similar to or exceeding $1.5h_{ef}$, but after the improvement, the fracture area of the anchor was smaller than $1.5h_{ef}$. Since the projected area (A_{Nco}) of the anchor fracture surface was the denominator in the cone fracture Eq. (1), the improved anchor design equation could have been underestimated. For this reason,

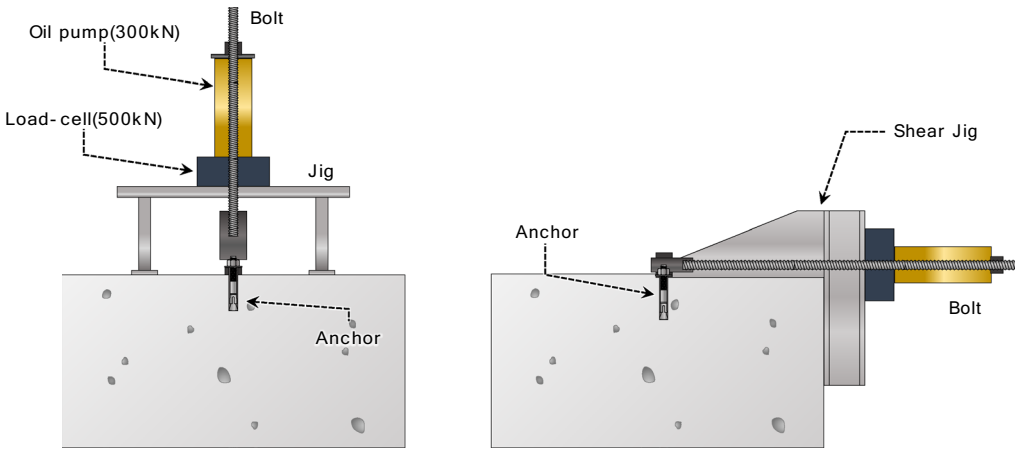

(a) Pull-out test set-up (b) Shear test set-up

Fig. 14 Anchor test set-up

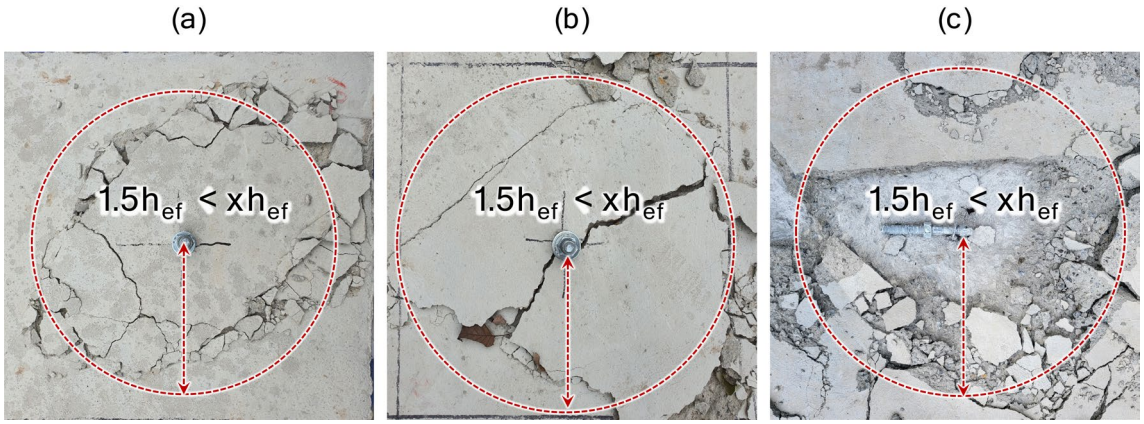

Fig. 15 Pull-out test results (before): **a** M12, **b** M16, **c** M20

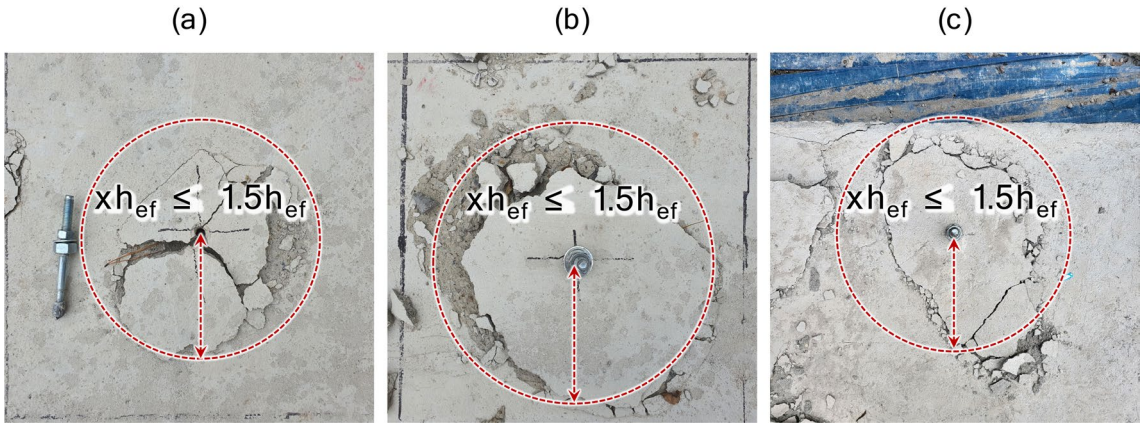

Fig. 16 Pull-out test results (after): **a** M12, **b** M16, **c** M20

Table 7 M12 Pull-out test results in normal-strength concrete

No.	Before						After					
	N[1]-50			N-70			N-50			N-70		
	Load (kN)	Displ (mm)	Failure mode[2]	Load (kN)	Displ (mm)	Failure mode[2]	Load (kN)	Displ (mm)	Failure mode[2]	Load (kN)	Displ (mm)	Failure mode[2]
1	31.8	4.2	CB	32.1	8.3	CB	33.7	4.7	CB	47.5	9.2	CB
2	23.9	3.7	CB	31.6	9.0	CB	32.8	4.4	CB	43.9	10.6	CB
3	28.1	4.5	CB	25.5	9.5	PF	35.0	4.6	CB	41.3	10.8	CB
4	22.7	4.1	CB	23.1	8.8	PF	28.4	4.6	CB	45.5	9.6	CB
5	22.1	2.3	CB	31.2	7.6	CB	30.3	1.9	CB	44.9	8.9	CB
Average	25.7	2.2		28.7	8.6		32.0	4.0		44.6	9.8	
Standard deviation		4.1			4.4			2.7			2.3	
Coefficient of variation		16.1%			15.1%			8.4%			5.1%	

[1] N: normal-strength concrete, [2]CB: concrete cone failure, PF: pull-out failure

Table 8 M12 pull-out test results in high-strength concrete

No.	Before						After					
	H[1]-50			H-70			H-50			H-70		
	Load (kN)	Displ (mm)	Failure mode[2]	Load (kN)	Displ (mm)	Failure mode[2]	Load (kN)	Displ (mm)	Failure mode[2]	Load (kN)	Displ (mm)	Failure mode[2]
1	26.7	5.0	CB	35.2	8.8	CB	32.84	5.1	CB	52.2	9.8	CB
2	25.2	3.2	PF	30.1	5.0	PF	31.7	4.6	CB	49.8	6.3	CB
3	26.1	5.2	PF	28.5	6.7	PF	33.71	5.23	CB	52.4	6.1	CB
4	23.9	4.6	CB	31.8	7.6	PF	36.04	4.35	CB	47.4	8.0	CB
5	28.1	5.1	CB	41.2	6.4	CB	31.46	4.37	CB	56.3	7.5	CB
Average	26.0	4.6		33.4	7.3		33.2	4.7		51.6	7.5	
Standard deviation		1.6			5.0			1.9			3.3	
Coefficient of variation		6.1%			15.1%			5.6%			6.4%	

[1] H: high-strength concrete, [2]CB: concrete cone failure, PF: pull-out failure

it is considered necessary to modify the design of the improved anchor.

The anchor with a 50 mm depth for normal-strength concrete before the improvement showed concrete cone breakage with all specimens. However, in high-strength concrete, three out of five specimens showed a concrete cone failure, and two specimens showed a pull-out failure. In the case of the 70 mm embedded depth for normal-strength concrete, three specimens showed a concrete cone failure, and two specimens showed a pull-out failure. In high-strength concrete, two specimens showed a concrete cone failure, and three specimens showed a pull-out failure.

In the case of normal-strength concrete before improvement, the average strength of the anchor with the embedded depth of 50 mm was 25.7kN, with a standard deviation of 4.1 and a coefficient of variation of 16.1%. Furthermore, the average strength of the anchor with the embedded depth of 70 mm was 28.7kN, with a standard deviation of 4.4 and a coefficient of variation of 15.1%. For the high-strength concrete, the average strength of the anchor with an embedded depth of 50 mm was 26.0kN, with a standard deviation of 1.6, and a coefficient of variation of 6.1%. The average strength of the anchor with an embedded depth of 70 mm was 33.4kN, with a standard deviation of 5.0, and a coefficient of variation of 15.1%. For the anchor before improvement, the coefficient of variation was large. This was because of a large deformation due to the open sleeve, resulting in a large loss in the keying and friction force, which in turn affects the pulling strength.

After the improvement, the normal-strength and high-strength concrete showed concrete cone failure patterns at depths of 50 mm and 70 mm. For normal-strength concrete, the average strength of the anchor with an embedded depth of 50 mm was 32.0kN, with a standard

deviation of 2.7, and a coefficient of variation of 8.4%. The average strength of the anchor with an embedded depth of 70 mm was 44.6kN, with a standard deviation of 2.3, and a coefficient of variation of 5.1%. For high-strength concrete, the average strength of the anchor with an embedded depth of 50 mm was 33.2kN, with a standard deviation of 1.9, and a coefficient of variation of 5.6%. The average strength of the anchor with an embedded depth of 70 mm was 51.6kN, with a standard deviation of 3.3, and a coefficient of variation of 6.4%. For the anchor after improvement, the coefficient of variation was lower than that of the anchor before improvement in both normal and high-strength concretes. The friction area likely increased due to an increase in the length of the header part, and the open part of the sleeve decreased, so the overall gripping force improved.

Tables 9 and 10 show the results according to the concrete strength before and after improvement for the M16 and M20 anchors. For the M16 anchor, two out of five normal-strength and high-strength concrete before improvement showed a concrete cone failure, and three showed a pull-out failure. However, after improvement, the anchor showed concrete cone failure in both normal-strength and high-strength concrete. The average strength of the normal-strength concrete anchor was 47.0kN, with a standard deviation of 4.5, and a coefficient of variation of 9.5%. The average strength of the high-strength concrete anchor was 61.4kN, with a standard deviation of 4.1, and a coefficient of variation of 6.6%. The final failure patterns of the normal-strength and high-strength concrete specimens to which the anchor was applied after the improvement showed a concrete cone failure pattern. The average strength of the normal-strength concrete anchor was 66.7kN, with a standard deviation of 3.3, and a coefficient of variation of 5.0%. The average strength of

Table 9 M16 pull-out test results in normal-strength and high-strength concrete

No.	Before			After			Before			After		
	N[1]-80			N-80			H-80			H-80		
	Load (kN)	Displ (mm)	Failure mode[2]	Load (kN)	Displ (mm)	Failure mode[2]	Load (kN)	Displ (mm)	Failure mode[2]	Load (kN)	Displ (mm)	Failure mode[2]
1	41.5	6.7	PF	69.4	8.8	CB	66.6	8.4	CB	83.6	11.0	CB
2	45.6	7.2	CB	68.3	7.8	CB	55.7	9.1	PF	81.5	9.8	CB
3	43.5	7.7	PF	63.1	10.9	CB	63.5	9.6	CB	79.4	13.6	CB
4	53.1	6.7	CB	70.5	10.8	CB	57.6	8.4	PF	87.3	13.5	CB
5	51.2	4.0	CB	62.4	8.6	CB	63.4	5.0	CB	77.9	10.7	CB
Average	47.0	6.5		66.7	9.4		61.4	8.1		81.9	11.7	
Standard deviation		4.5			3.3			4.1			3.3	
Coefficient of variation		9.5%			5.0%			6.6%			4.0%	

[1] N: normal-strength concrete, [2]CB: concrete cone failure, PF: pull-out failure

Table 10 M20 Pull-out test results in normal-strength and high-strength concrete

No.	Before			After			Before			After		
	N[1]-100			N-100			H-100			H-100		
	Load (kN)	Displ (mm)	Failure mode[2]	Load (kN)	Displ (mm)	Failure mode[2]	Load (kN)	Displ (mm)	Failure mode[2]	Load (kN)	Displ (mm)	Failure mode[2]
1	75.2	9.5	PF	79.9	13.6	CB	81.4	12.4	PF	91.0	20.7	CB
2	92.5	14.4	CB	84.9	20.6	CB	100.6	10.5	CB	99.2	17.5	CB
3	90.5	9.7	CB	85.5	13.8	CB	82.1	9.8	PF	93.7	16.3	CB
4	71.1	9.6	PF	83.5	13.7	CB	103.2	12.1	CB	92.7	20.1	CB
5	77.2	8.9	PF	81.6	12.7	CB	80.1	11.0	PF	92.9	18.4	CB
Average	81.3	10.4		83.1	14.9		89.5	11.2		93.9	18.6	
Standard deviation		8.6			2.1			10.2			2.8	
Coefficient of variation		10.6%			2.5%			11.4%			3.0%	

[1] N: normal-strength concrete, [2]CB: concrete cone failure, PF: pull-out failure

the high-strength concrete anchor was 81.9kN, with a standard deviation of 3.3, and a coefficient of variation of 4.0%.

For the M20 anchor, two out of five normal-strength and high-strength concrete specimens before improvement showed concrete cone failure, and three showed a pull-out failure pattern. However, after improvement, the anchor showed concrete cone failure in both normal-strength and high-strength concretes. The average strength of the normal-strength concrete anchor was 81.3kN, with a standard deviation of 8.6, and a coefficient of variation of 10.6%. The average strength of the high-strength concrete anchor was 89.5kN, with a standard deviation of 10.2, and a coefficient of variation of 11.4%. The final failure pattern of the normal-strength and high-strength concrete specimens to which the anchor was applied after the improvement showed a concrete cone failure pattern. The average strength of the normal-strength concrete anchor was 83.1kN, with a standard deviation of 2.1, and a coefficient of variation of 2.5%. The average strength of the high-strength concrete anchor was 93.9kN, with a standard deviation of 2.8, and a coefficient of variation of 3.0%.

Fig. 17 shows the relative ratio of the pull-out strength of the M12 anchor according to the embedded depth before and after the improvement. As shown in this figure, in the case of normal-strength concrete, the pull-out strength before and after the improvement increased by 1.25 times when the embedded depth was 50 mm, and increased by 1.56 times when the embedded depth was 70 mm. For the high-strength concrete, the pull-out strength before and after the improvement increased by 1.28 times when the embedded depth was 50 mm, and increased by 1.55 times when the embedded depth was 70 mm.

Fig. 18 shows the relative ratios of the pull-out strengths of the M16 and M20 anchors according to the concrete strength before and after the improvement. For the M16 anchor, normal-strength concrete showed an increase of about 1.42 times, and high-strength concrete increased by about 1.33 times. In addition, the M20 anchor showed similar results. In the finite element analysis, the strength before and after the improvement was about 225%. In the results, it ranged from 125 to 155%, depending on the embedded depth. This result is proposed to be caused by various problems (verticality and clearness) that might have occurred during construction. However, when the sleeve and header of the anchor were improved, the standard deviation of each anchor was uniform, and the value of the coefficient of variation satisfied the value required by regulations.

Figs. 19 and 20 show the final failures of the anchor shear tests before and after improvement. Tables 11, 12, and 13 show the shear test results of the anchors before and after the improvement for each diameter.

For the M12 anchor, the average shear strength before improvement was 18.1kN, with a standard deviation of 3.2, and a coefficient of variation of 17.7%. The average strength of the anchor after improvement was 25.1kN, with a standard deviation of 1.8, and a coefficient of variation of 7.1%. For the anchor after improvement, the coefficient of variation was stable, as in the pull-out strength test. An improvement of about 138% in seismic performance was found upon comparing the internal force before and after the improvement.

The average shear strength of the M16 anchor before improvement was 26.8kN, with a standard deviation of 2.6, and a coefficient of variation of 9.5%. The average shear strength of the M16 anchor after improvement was 38.8kN, with a standard deviation of 2.0, and a coefficient

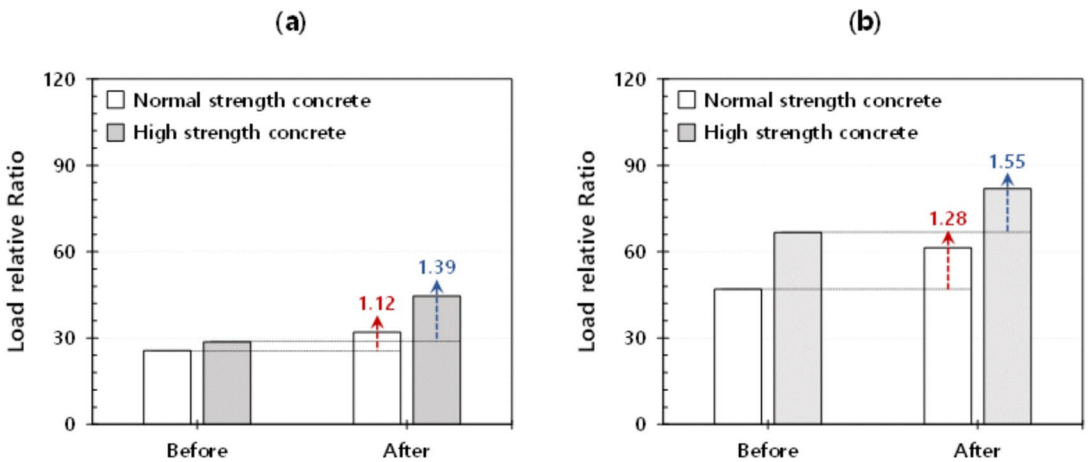

Fig. 17 M12 tensile strength ratio according to the embedded depth: **a** 50 mm, **b** 70 mm

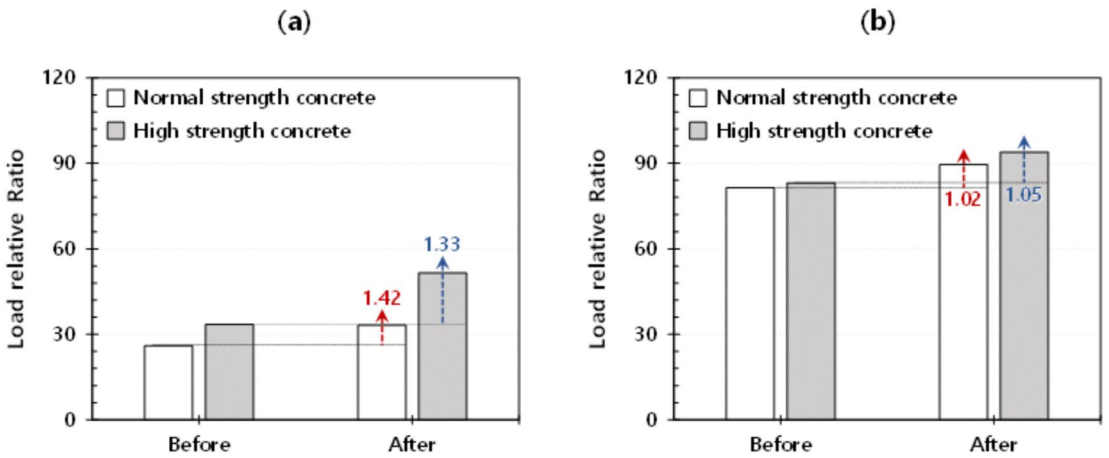

Fig. 18 Tensile strength ratio according to concrete strength: **a** M16, **b** M20

(a) M12 (b) M16 (c) M20

Fig. 19 Shear test results (before)

(a) M12 (b) M16 (c) M20

Fig. 20 Shear test results (after)

Table 11 M12 shear test results (normal-strength concrete)

No.	Before			After		
	N-70			N-70		
	Load (kN)	Displ (mm)	Failure mode[1]	Load (kN)	Displ (mm)	Failure mode[1]
1	18.4	29.1	SF	26.0	46.4	PF
2	16.6	40.1	SF	23.3	27.0	PF
3	22.6	23.1	SF	23.6	33.0	PF
4	13.9	22.1	SF	24.8	27.9	PF
5	19.1	30.1	SF	27.6	42.8	PF
Average	18.1	28.9		25.1	35.4	
Standard deviation		3.2			1.8	
Coefficient of variation		17.7%			7.1%	

[1] SF: steel failure, PF: pry-out failure

Table 12 M16 shear test results (normal-strength concrete)

No.	Before			After		
	N-80			N-80		
	Load (kN)	Displ (mm)	Failure mode[1]	Load (kN)	Displ (mm)	Failure mode[1]
1	26.9	39.7	PF	36.9	56.7	PF
2	23.1	28.6	SF	42.1	40.8	PF
3	25.0	22.0	SF	40.2	31.4	PF
4	28.9	23.7	PF	37.1	33.8	PF
5	30.2	20.5	PF	37.7	29.3	PF
Average	26.8	26.9		38.8	38.4	
Standard deviation		2.6			2.0	
Coefficient of variation		9.5%			5.2%	

[1] SF: steel failure, PF: pry-out failure

Table 13 M20 shear test results (normal-strength concrete)

No.	Before			After		
	N-80			N-80		
	Load (kN)	Displ (mm)	Failure mode[1]	Load (kN)	Displ (mm)	Failure mode[1]
1	50.1	37.8	SF	65.6	54.1	PF
2	48.1	39.6	SF	60.9	56.6	PF
3	67.2	36.3	SF	62.6	51.9	PF
4	45.2	27.2	SF	61.7	38.9	PF
5	46.5	32.4	SF	54.7	46.3	PF
Average	51.4	34.7		61.1	49.5	
Standard deviation		8.1			3.6	
Coefficient of variation		15.7%			5.8%	

[1] SF: steel failure, PF: pry-out failure

of variation of 5.2%. An improvement of 145% in seismic performance was also found upon comparing the internal force before and after improvement.

The average shear strength of the M20 anchor before the improvement was 51.4kN, with a standard deviation of 8.1, and a coefficient of variation of 15.7%. The average shear strength of the M20 anchor after the improvement was 61.1kN, with a standard deviation of 3.6, and a coefficient of variation of 5.8%. An improvement of about 119% in seismic performance was also found upon comparing the internal force before and after improvement.

5 Review and Suggestions for the Design Equation for an Extreme Pull-Out Load

The European Technical Approval Guideline (ETAG) (Committee et al., 2011; Tsavdaridis et al., 2016) and ACI (Institute and (ACI) Committee, Evaluating the Performance of Post-installed Mechanical Anchors in Concrete, 2019; Committee et al., 2019; Korean Building Code and Commentary (KBC) 2016) define the design criteria for each failure mode of the post-installed single anchor according to the pull-out load using an empirical formula based on failure strength experiments. According to ANCHORING TO CONCRETE: The New ACI approach (Karmazinova et al., 2009), the failure strength of the concrete cone, which appeared as the dominant failure mode in this research, was reported to be affected by the effective embedding depth ($1.5h_{ef}$) and concrete strength ($0.5f_{ck}$). In this study, the experimental values and design equations were compared and analyzed based on the design equation of Committee et al. (2011); Tsavdaridis et al., 2016).

5.1 European Technical Approval Guideline (ETAG)

5.1.1 Comparison of the Existing Equation and Test Values

Equation (3) shows the failure strength of concrete, which is not affected by the edge distance and anchor spacing in ETAG (Committee et al., 2011; Tsavdaridis et al., 2016) non-cracked concrete. Fig. 21 shows the comparison of the difference between the proposed ETAG (Committee et al., 2011; Tsavdaridis et al., 2016) formula and the actual test values:

$$N_{\mathrm{Ru,c}} = 14.6 \times \sqrt{f_{\mathrm{ck}}} \times {h_{\mathrm{ef}}}^{1.5}. \tag{3}$$

As shown in Fig. 21 the correlation coefficient between the design value and the test value of ETAG was 0.908, indicating that the value according to the experimental results partially satisfied the equation proposed by ETAG (Committee et al., 2011; Tsavdaridis et al., 2016). However, the coefficient of variation of the two values was 18.9%, which was relatively large. Since the design equation in ETAG (Committee et al., 2011; Tsavdaridis et al., 2016) only considers the effective embedded depth, even if the diameter of the anchor changes, the extreme pull-out load that is calculated is the same when the embedded depth is similar. This was not consistent with the results of this experiment, so it is necessary to consider the diameter in the design equation.

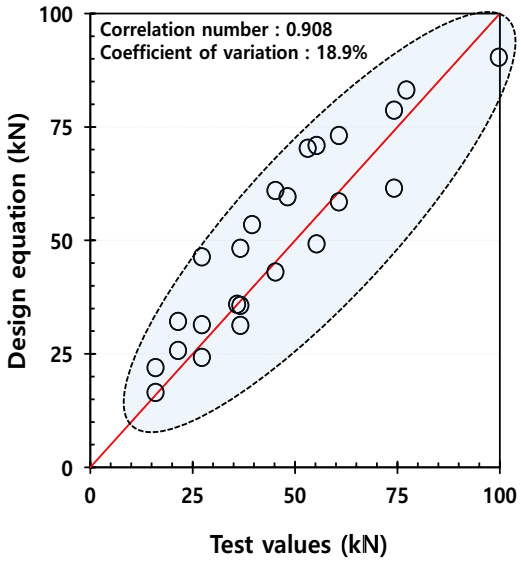

Fig. 21 Comparison of design equation and test values

5.2 Modified Equation

Equation (4) shows the proposed equation reflecting the effective embedded depth of the anchor and the diameter of the anchor:

$$N''_{\mathrm{Ru,c}} = 11.0 \times \sqrt{f_{\mathrm{ck}}} \times h_{\mathrm{ef}}^{0.9} \times d^{1.1}, \tag{4}$$

where $N''_{\mathrm{Ru,c}}$ denotes the extreme pull-out load; f_{ck} denotes the concrete compressive strength of the D10×20 specimen; d denotes the diameter of the anchor; and h_{ef} denotes the effective embedded depth.

Since the existing Eq. (3) does not reflect the diameter of the anchor, the extreme pull-out load was proportional to a 1.5 square of the effective embedded depth. According to the experimental results in this study, the extreme pull-out load increased as the diameter of the anchor increased, so the effect of the effective embedded depth appeared to be close to a linear relationship. The effect of the effective embedded depth on the extreme pull-out load was excessively reflected because the diameter of the anchor was not reflected in the existing Eq. (3). Fig. 22p shows the correlation between Eq. (4) and the extreme pull-out load obtained from the experiment. The correlation coefficient was 0.972, which is higher than that of the existing Eq. (3), and at the same time, the coefficient

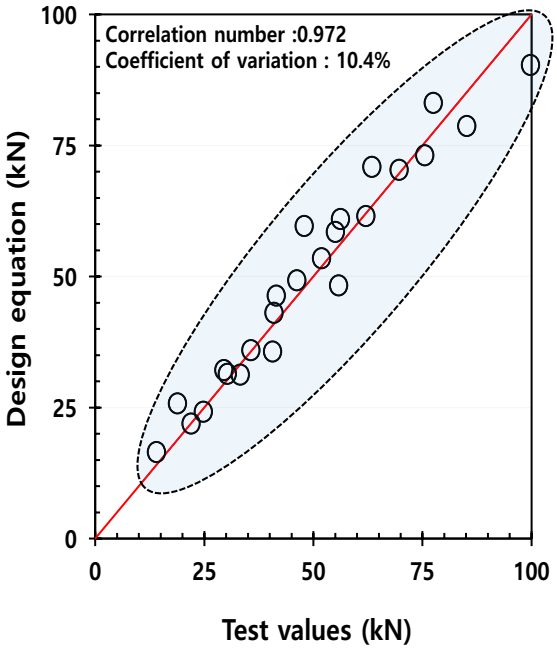

Fig. 22 Comparison of the design equation and test values

of variation was also reduced to 10.4%, which was less than the 18.9% of the existing equation. Therefore, Eq. (4) more accurately reflected the actual experimental value than the existing Eq. (3).

6 Conclusion

This research assesses the improvements in the head and extension sleeve of an existing post-installed anchor. The length of the extension sleeve and header of the post-installed anchor was determined via finite element analysis. The performance of the anchor before the improvement was compared and evaluated using the pull-out and shear performance tests of the proposed post-installed anchor. In addition, the suitability of the anchor strength design equation was evaluated according to the embedded depth of the proposed post-installed anchor, the diameter of the anchor, and the concrete strength. The conclusions are as follows:

1. A post-installed anchor was proposed with an improved sleeve length and header length. The optimal sleeve length (9.0mm) and header length (3.0mm) were selected via FEM analyses. As a result, the performance improved by 1.71 times compared to the existing model. Therefore, it was found that the performance of the post-installed anchor improves when the sleeve length and header length are enhanced.
2. The pull-out strength test showed that the projected area of concrete cone failure of the anchor before improvement exceeded $1.5h_{ef}$, but the cone failure area of the anchor after improvement was $1.5h_{ef}$ or less. These results should be reflected in the anchor design equation.
3. The improved pull-out strength test of M12 showed an increase of 1.25 times in normal-strength concrete and 1.28 times in high-strength concrete, with an embedded depth of 50mm. In addition, in normal-strength and high-strength concretes with an embedded depth of 70mm, the increase was 1.55 times. The test for the improved pull-out strength of M12 showed an increase of 1.38 times. The improved pull-out strength test of M16 showed that the pull-out strength increased by 1.42 times for normal-strength concrete and 1.33 times for high-strength concrete.
4. For the strength calculating equation presented by ETAG, the extreme pull-out load for concrete failure was determined by the effective embedded depth and the concrete compressive strength without considering the diameter. Therefore, this research proposes a modified equation that reflects changes in effective embedded depth and diameter. A comparison of the proposed equation with that of ETAG showed that the correlation coefficient changed from 0.908 to 0.962, and the coefficient of variation changed from 18.9% to 10.4%, meaning that the proposed equation reflected the actual experimental values more accurately.

Acknowledgements
This work was supported by Basic Science Research Program through the National Research Foundation of Korea (NRF-2018R1A6A1A07025819, NRF-2022R1I1A1A0106389911).

Author Contributions
Conceptualization,H.-H.L. M.-W.H. and T.-W.P.; methodology, K.-H.C. M.-W.H. and T.-W.P.; validation, H.-H.L. M.- W.H. and T.-W.P.; formal analysis, M.-W.H. and K.-H.C.; investigation, K.-H.C. M.-W.H.; analysis, M.-W.H. and K.- H.C.; resources, M.-W.H. and T.-W.P.; data curation, M.-W.H. and H.-H.L.; writ-ing—original draft preparation, M.- W.H.; writing—review and editing, M.-W.H. and T.-W.P.; visualization, M.-W.H. and T.-W.P.; super-vision, T.-W.P.; project administration, M.-W.H.; project administration, M.-W.H. and T.-W.P.

Funding
This work was supported by Basic Science Research Program through the National Research Foundation of Korea (NRF-2018R1A6A1A07025819, NRF-2022R1I1A1A0106389911).

Availability of data and materials
We will provide the data whenever we contact the corresponding author.

Declarations

Competing Interests
The authors declare no competing interests.

Received: 22 September 2023 Accepted: 9 August 2024
Published: 6 January 2025

References

ACI Committee. (2011). Building code requirements for structural concrete and commentary (ACI 318–11), American Concrete Institute.
ACI Committee. (2019). Building code requirements for structural concrete (ACI 318-19) and Commentary, American Concrete Institute.
Alhaidary, H., & Al-Tamimi, A. (2021). Importance of performance certification for post-installed anchors: An experimental assessment. *Structures., 29*, 273–285. https://doi.org/10.1016/j.istruc.2020.11.005
American Concrete Institute (ACI) Committee. (2019). Evaluating the performance of post-installed mechanical anchors in concrete (ACI 355.2-19), American Concrete Institute.
Bang, J. S., Youn, I. R., Kwon, Y. S., & Yim, H. J. (2020). Nonlinear tensile behavior analysis of torque-controlled expansion anchors using finite element analysis. *Journal of Korea Institute for Structural Maintenance and Inspection., 24*, 91–99. https://doi.org/10.11112/jksmi.2020.24.4.91
Breen, E., Eichinger, E. M., & Fuchs, W. (2001). Anchoring to concrete: The new ACI approach. In R. Eligehausen (Ed.), *International Symposium on Connections between Steel and Concrete* (pp. 31–44). RILEM Publications SARL.
Chen, Z., Nassiri, S., Lamanna, A., & Cofer, W. (2020). Investigation of pull-through and pullout failure modes of torque-controlled expansion anchors. *ACI Structural Journal*. https://doi.org/10.14359/51716807
Dassault Systemes. (1978). ABAQUS, Version 6.20, ABQUS Inc, February 1, 1978. http://plm.vpkcorp.com/_plm/
Delhomme, F., Pallud, B., & Rouane, N. (2018). Tightening torque influence on pullout behavior of post-installed expansion anchors. *KSCE Journal of Civil Engineering, 22*(2018), 3931–3939. https://doi.org/10.1007/s12205-018-0930-9
ETAG. (2003). Guideline for European technical approval of metal anchors for use in concrete.
European Technical Approval Guideline (ETAG). (1997). Guideline for European technical approval of metal anchors for use in concrete.
Gontarz, J., & Podgorski, J. (2019). Analysis of crack propagation in a "pull-out" test. *Studia Geotechnica Et Mechanica., 41*, 160–170. https://doi.org/10.2478/sgem-2019-0015
Karmazinova, M., Melcher, J., & Kala, Z. (2009). Design of expansion anchors to concrete based on results of experimental verification. *Advanced Steel Construction., 5*, 390–405.
Kim, J. S., Jung, W. Y., Kwon, M. H., & Ju, B. S. (2013). Performance evaluation of the post-installed anchor for sign structure in South Korea. *Construction and Building Materials., 44*, 496–506. https://doi.org/10.1016/j.conbuildmat.2013.03.015
Korean Building Code and Commentary (KBC). (2016). Architectural Institute of Korea, Standards for structural design, construction and safety of buildings and structures, Seoul, KBC.
Lubliner, J., Oliver, J., Oller, S., & Onate, E. (1989). A plastic-damage model for concrete. *International Journal of Solids and Structures., 25*, 299–326. https://doi.org/10.1016/0020-7683(89)90050-4
Pishro, A., Feng, X., Ping, Y., Dengshi, H., & Shirazinejad, R. (2020). Comprehensive equation of local bond stress between UHPC and reinforcing steel bars. *Construction and Building Materials, 262*, 119942. https://doi.org/10.1016/j.conbuildmat.2020.119942
Siamakani, S., Nagai, K., Jiradilok, P., & Sahamitmongkol, R. (2022). Prevention of concrete breakout failure of expansion anchor in tension by post-installed reinforcement: Discrete analysis and experiment. *CSCM., 17*, e01233. https://doi.org/10.1016/j.cscm.2022.e01233
Tsavdaridis, K. D., Shaheen, M. A., Baniotopoulos, C., & Salem, E. (2016). Analytical approach of anchor rod stiffness and steel base plate calculation under tension. *Structures., 5*, 207–218. https://doi.org/10.1016/j.istruc.2015.11.001

Publisher's Note

Moo-Won Hur Professor, Department of Smart Architecture Engineering, Dongyang University, Yeongju-si Republic of Korea

Kyoung-Hun Chae Doctor's course, Department of Architectural Engineering, Dankook University, Yongin, Republic of Korea

Hyun-Ho Lee Professor, Department of Smart Architecture Engineering, Dongyang University, Yeongju-siRepublic of Korea

Tae-Won Park Professor, Department of Architectural Engineering, Dankook University, Yongin, Republic of Korea